Korean J. Chem. Eng., **28**(12), 2319-2323 (2011)
DOI: 10.1007/s11814-011-0112-7

Solubility of hinokitiol in supercritical fluids; measurement and correlation

Junhyuk Lim*, Hwayong Kim*, Hye Kyung Cho, and Moon Sam Shin**,†**

*School of Chemical & Biological Engineering, Seoul National University, Seoul 151-744, Korea
**Department of Dermatological Health Management, Eulji University,
212 Yangji-dong, Sujeong-gu, Seongnam-si, Gyeonggi-do 461-713, Korea
(*Received 9 November 2010 • accepted 24 April 2011*)

Abstract−Supercritical fluid technology has been an alternative for purification and separation of biological compounds in cosmetic, food, and pharmaceutical products. Solubility information of biological compounds in supercritical fluids is essential for choosing a supercritical fluid processes. The equilibrium solubility of hinokitiol was measured in supercritical carbon dioxide and ethane with a static method in the pressure range from 8 to 40 MPa and at temperatures equal to 313.2, 323.2 and 333.2 K. The experimental data were correlated well by Peng-Robinson equation of state and quasi-chemical nonrandom lattice fluid model.

Key words: Supercritical Fluids, Hinokitiol, Carbon Dioxide, Ethane, Solubility

INTRODUCTION

Hinokitiol (2-Hydroxy-6-propan-2-ylcyclohepta-2,4,6-trien-1-one, $C_{10}H_{12}O_2$, CAS No. 449-44-5) is known as β-thujaplicin and its chemical structure is shown in Fig. 1. It is a troplone-related compound found in the heartwood of cupressaceous plants that possesses a wide range of biochemical and pharmacological attributes such as anti-inflammatory [1], anti-fungal [2], anti-bacterial [3], anti-tumor [4], antioxidant [5], reducing of melanin content [6], and apoptosis [7]. The drugs must be dissolved in water in order to be absorbed and to exert their effects. The bioavailability of the drug, the percentage of the drug absorbed compared to its initial dose, is limited by insolubility such as hinokitiol. Micronization of the drug can enhance a drug's dissolution rate in the biologic environment. Dissolution rate is a function of solubility as well as particle surface area wherein the surface area can be increased through a reduction of particle size.

Supercritical fluid technology has emerged as an important technique for various applications, including extraction and purification of cosmetics and pharmaceuticals, micronization of the drug, powder processing, pollution prevention, crystallization processes, bioseparations, food processing, polymerizations, chemical reaction, cleansing of semiconductors and precision machinery [8]. Supercritical fluid extraction is an alternative to liquid extraction using solvents such as hexane or dichloromethane. There will always be some residual solvent left in the extract and matrix, and there is always some level of environmental contamination from their use. In contrast, supercritical fluids are easy to remove simply by reducing the pressure, leaving almost no trace, and purchased supercritical fluids have almost always been reclaimed, which reduces the total carbon footprint. Supercritical carbon dioxide [8], in particular, has many advantages such as moderate critical temperature, nontoxicity, inexpensive, high diffusivity, low surface tension, low viscosity and good density, which is essential in enabling the solvent to readily penetrate solid biomass matrix as well as in extracting the biomaterials. Supercritical ethane [9] is also used in supercritical extraction since it has relatively low critical temperature (305.3 K), which is similar to that of carbon dioxide (304.2 K) and no damage to the function properties of the extracts.

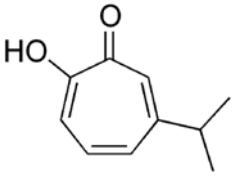

Fig. 1. Chemical structure of hinokitiol.

Solubility information of biological compounds is crucial for choosing supercritical fluid processes in extraction, purification, and particle design. Measurements of solubility in supercritical fluid are divided into static method [10], flow-through method [11] and recirculation systems [12]. Static method with variable volume view cell is very convenient and it can be effectively used for solids that exhibit higher solubility than 10^{-5} mole fraction [13]. In flow method, the vessel is filled with a solute, and a supercritical fluid continuously flows through the vessel. Recirculation systems use a constant volume equilibrium vessel which is continuously recirculated until equilibrium and solid solubility is measured with on-line high pressure liquid chromatography or coupled UV-vis spectrophotometer.

Thermodynamic modeling of SCF phase equilibria has been reviewed by Brennecke and Eckert [14]. Correlations of solid solubility containing biological compounds in supercritical fluids were presented using Peng-Robinson (PR) equation of state (EOS) [15], solution model [16] and Sanchez-Lacombe lattice model [17]. Most recently, the present authors presented a quasi-chemical nonrandom lattice fluid (QLF) model [18] and found that the model EOS successfully modeled the phase behavior of classical pure fluids

†To whom correspondence should be addressed.
E-mail: msshin@eulji.ac.kr

and mixtures containing non-associating and associating molecules [19,20], solubility of polymer in supercritical carbon dioxide [21], and the solubility of biological compounds in supercritical fluid [22-24].

In this study, the equilibrium solubility of hinokitiol in supercritical carbon dioxide and ethane was measured with a static method using a high pressure apparatus installed in a variable volume view cell in the pressure range from (8 to 40) MPa and at temperatures of (313.2, 323.2 and 333.2) K. The experimental data were correlated by the PR EOS [25] and the QLF EOS [18].

EXPERIMENTAL SECTION

1. Materials

Carbon dioxide (min. 99.5%) and ethane (min. 99.5%) were supplied from Korea Industrial Gases. Hinokitiol (min. 98.0%) were supplied by Osaka Corporation. These materials were used without further purification.

2. Solubility Apparatus and Procedure

The cloud points of hinokitiol in supercritical carbon dioxide and ethane were measured with a high pressure apparatus installed a variable volume view cell. In our previous studies, this apparatus was used to measure solubility of polymer in supercritical carbon dioxide [21,26] and solubility of biocides in supercritical fluid [22-24]. Fig. 2 shows a schematic diagram of the experimental apparatus; the view cell is constructed with high nickel-content austenitic steel (5.7 cm o.d., 1.59 cm i.d., 25 cm^3 working volume). This apparatus and procedure has been described in detail in our previous researches [21-24,26]. The measured amount of hinokitiol was loaded into the cell and then carbon dioxide was added to the cell. The solution in the cell was agitated and heated to the desired temperature. After the solution reached and was maintained as a single phase, the pressure was slowly reduced by moving the piston located within the cell using the pressure generator until the solution became cloudy. The solubility of hinokitiol in supercritical fluid was determined by observing the cloud point, which is defined as the pressure at which it is no longer possible to observe the magnetic bar [21-24,26]. This procedure was repeated several times until the fluctuation of phase transition pressure was minimized to within ±0.01 MPa.

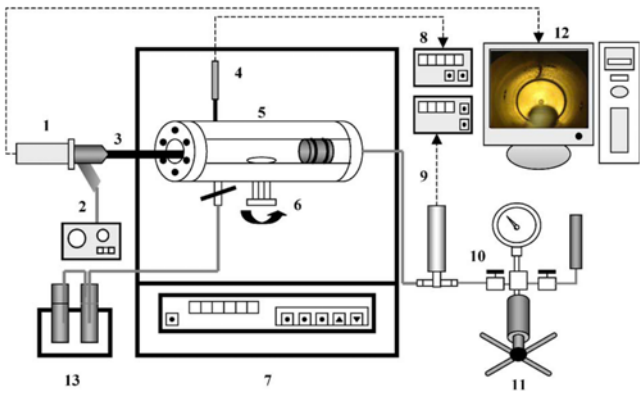

Fig. 2. Schematic diagram of experimental apparatus.

1. Camera
2. Light source
3. Borescope
4. Fast response PRT
5. Viewcell
6. Magnetic stirrer
7. Air bath
8. Digital thermometer
9. Digital pressure transducer
10. Pressure gauge
11. Hand pump
12. Computer monitor
13. Trap

CORRELATION

Experimental data obtained in this study were correlated with the Peng-Robinson (PR) EOS [25] and the quasi-chemical nonrandom lattice fluid (QLF) EOS [18].

The PR EOS was as follows:

$$p = \frac{RT}{V-b} - \frac{a(T)}{V(V+b)+b(V-b)} \tag{1}$$

The van der Waals one fluid mixing rules used in this study were given by

$$a = \sum_i \sum_j x_i x_j a_{ij} \tag{2}$$

$$b = \sum_i x_i b_i \tag{3}$$

$$a_{ij} = \sqrt{a_i a_j}(1-k_{ij}) \tag{4}$$

where k_{ij} is the binary interaction parameter.

The QLF EOS and the fugacity coefficient of a component in mixture are given by

$$\frac{\tilde{p}}{\tilde{T}} = -\ln(1-\tilde{\rho}) + \frac{z}{2}\ln\left[1+\left(\frac{q}{r}-1\right)\tilde{\rho}\right] - \frac{\theta^2}{\tilde{T}} \tag{5}$$

$$\ln\varphi_i = (Z-1)\frac{r_i}{r}\left(\frac{v_i^*}{v^*}-1\right) + r_i\frac{\tilde{p}}{\tilde{T}} - \frac{zq_i}{2}\ln\left(1+\left(\frac{q}{r}-1\right)\tilde{\rho}\right) - \ln Z$$
$$+ \frac{q_i\theta}{\tilde{T}}\left[\theta - \frac{2\sum_{j=0}^{c}\theta_j\varepsilon_{ij} + \beta\sum_{j=0}^{c}\sum_{k=0}^{c}\sum_{l=0}^{c}\theta_j\theta_k\theta_l\varepsilon_{ij}(\varepsilon_{ij}+2\varepsilon_{kl}-2\varepsilon_{jk}-2\varepsilon_{ik})}{\theta\varepsilon_M}\right] \tag{6}$$

where ε_M, ε_{ij} are defined by

$$\varepsilon_M = \frac{1}{\theta^2}\left[\sum_{i=0}^{c}\sum_{j=0}^{c}\theta_i\theta_j\varepsilon_{ij} + \frac{\beta}{2}\sum_{i=0}^{c}\sum_{j=0}^{c}\sum_{k=0}^{c}\sum_{l=0}^{c}\theta_i\theta_j\theta_k\theta_l\varepsilon_{ij}(\varepsilon_{ij}+3\varepsilon_{kl}-2\varepsilon_{ik}-2\varepsilon_{jk})\right] \tag{7}$$

$$\varepsilon_{ij} = \sqrt{\varepsilon_{ii}\varepsilon_{jj}}(1-k_{ij}) \tag{8}$$

RESULTS AND DISCUSSION

In our previous studies [23], we tested successfully our solubility measurement apparatus and showed good agreement with the literature data at relatively high solubility with over the order 10^{-4} mole fraction. The solubility data of hinokitiol in supercritical carbon dioxide and ethane was measured by observing a cloud point at temperatures of 313.2, 323.2 and 333.2 K. The solubility of hinokitiol in supercritical carbon dioxide and ethane is given in Tables 1 and 2, respectively. In both systems, solubility increased as pressure increased at a constant temperature due to higher density of the supercritical fluids and higher specific interaction between the solute and supercritical fluids.

Table 1. Experimental data of hinokitiol solubility in supercritical carbon dioxide at 313.2, 323.2 and 333.2 K

T (K)	p (MPa)	$y_2 \times 10^4$
313.2	10.14	5.91
	11.81	8.80
	13.53	12.52
	15.28	13.99
	19.57	17.01
	23.52	18.83
	27.81	19.71
	32.67	20.29
	37.83	21.82
323.2	12.21	5.91
	13.54	8.80
	14.84	12.52
	15.98	13.99
	17.29	17.01
	19.03	18.83
	20.54	19.71
	22.98	20.29
	26.84	21.82
	33.17	23.51
333.2	14.23	5.91
	15.51	8.80
	16.67	12.52
	17.92	13.99
	19.94	17.01
	20.53	18.83
	21.59	19.71
	22.58	20.29
	23.52	21.82
	28.74	23.51
	35.84	24.90

Table 2. Experimental data of hinokitiol solubility in supercritical ethane at 313.2, 323.2 and 333.2 K

T (K)	p (MPa)	$y_2 \times 10^4$
313.2	8.04	5.81
	10.02	8.32
	12.86	11.60
	14.98	14.25
	18.39	17.79
	21.39	9.08
	24.94	20.82
	31.32	22.68
	36.97	23.87
323.2	8.54	5.81
	9.33	8.32
	11.03	11.60
	12.49	14.25
	14.81	17.79
	16.42	19.08
	18.71	20.82
	21.53	22.68
	26.17	23.87
	35.15	27.31
333.2	9.56	5.81
	10.27	8.32
	11.43	11.60
	13.12	14.25
	15.36	17.79
	16.45	19.08
	17.83	20.82
	20.62	22.68
	22.52	23.87
	25.74	27.31
	31.64	31.80
	38.84	35.70

PR EOS requires three pure parameters: critical temperature, critical pressure, acentric factor. The properties of the pure CO_2, ethane and hinokitiol in PR EOS are listed in Table 3. The critical properties of hinokitiol were estimated from group contribution method, developed by Stein and Brown [27]. The sublimation pressures and molar volume of hinokitiol could be calculated by group contribution method [28,29]. QLF EOS needs three molecular parameters: unit cell volume (v_i^*), segment number (r_i), and energy parameter (ε_{ii}). Pure parameters of carbon dioxide and ethane in QLF EOS are fitted to saturated liquid density, vapor pressure and p-V-T data from the Korea Thermophysical Properties Databank (KDB) [30].

Pure parameters of hinokitiol in QLF EOS are fitted to vapor pressure from group contribution method [27]. Molecular parameters for pure carbon dioxide and ethane in QLF EOS are described in Table 4. Binary interaction parameter k_{ij} was obtained by minimizing the absolute average deviation of y_2 (AADy):

$$\mathrm{AADy} = \frac{1}{N_{exp}} \sum_{i}^{N_{exp}} \left| \frac{y_{2i}^{exp} - y_{2i}}{y_{2i}^{exp}} \right| \tag{9}$$

where y_{2i}^{exp}, y_{2i} are, respectively, the experimental solubility of the solid in supercritical fluids and that calculated by means of EOS.

Table 3. Pure properties of pure carbon dioxide, ethane and hinokitiol

Components	T_c (K)	p_c (MPa)	ω	v^s (cm^3 mol^{-1})	$A^{sbu,a}$	$B^{sub,a}$	Reference or estimation method
Carbon dioxide	304.2	7.38	0.224	-	-	-	KDB [26]
Ethane	305.3	4.87	0.100	-	-	-	KDB [26]
Hinokitiol	803.1	3.78	0.760	180.1	9.797	4644.7	Group contribution method [22-25]

[a] $\log p^{sub}$ (bar) $= A^{sub} - B^{sub}/T$

Table 4. Molecular parameters for pure carbon dioxide, ethane and hinokitiol in QLF EOS

Components	v_i^* ($cm^3\ mol^{-1}$)	r_i	ε_{ii}/k (K)
Carbon dioxide	4.016	7.520	68.40
Ethane	8.517	5.890	73.38
Hinokitiol	20.482	9.253	178.38

Table 5. Binary interaction parameters, of the PR, QLF EOS and AADy for the carbon dioxide+hinokitiol and ethane+hinokitiol systems

Systems	T (K)	PR EOS		QLF EOS	
		k_{ij}	AADy	k_{ij}	AADy
Carbon dioxide	313.2	0.2186	0.2611	0.0527	0.1262
+hinokitiol	323.2	0.2249	0.1968	0.0649	0.1027
	333.2	0.2314	0.1289	0.0830	0.1023
Ethane	313.2	0.1874	0.1809	0.0175	0.0827
+hinokitiol	323.2	0.1919	0.2160	0.0275	0.0579
	333.2	0.2117	0.1548	0.0439	0.0452

The experimental data for the carbon dioxide+hinokitiol and ethane +hinokitiol systems were correlated with the PR EOS and the QLF EOS. The binary interaction parameters for these systems are summarized in Table 5 together with AADy. While the PR EOS fitted the experimental data within 26.11%, 21.60% AADP for carbon dioxide+hinokitiol and ethane+hinokitiol systems, respectively, the QLF EOS correlated well with them within 12.62%, 8.27% AADP for both systems, respectively. In both systems, the binary interaction parameters of PR and QLF EOS increased as temperature increased. In Figs. 3 and 4, the QLF EOS has better calculated results with the measured data for both systems than the PR EOS because the critical parameters for hinokitiol in PR EOS were estimated from group contribution method. By the way, near the critical region both models could not describe quantitatively the experimental data in these systems so the experimental data of biomaterials in supercritical fluids is essential for accurate modeling of phase behavior near the critical region.

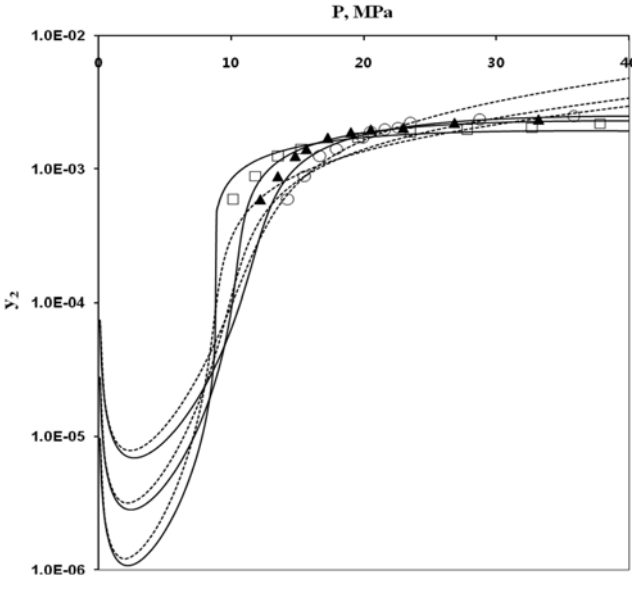

Fig. 3. Solubility of hinokitiol in supercritical carbon dioxide with the PR (dotted line) and QLF EOS (solid line): □, 313.2 K; ▲, 323.2 K; ○, 333.2 K.

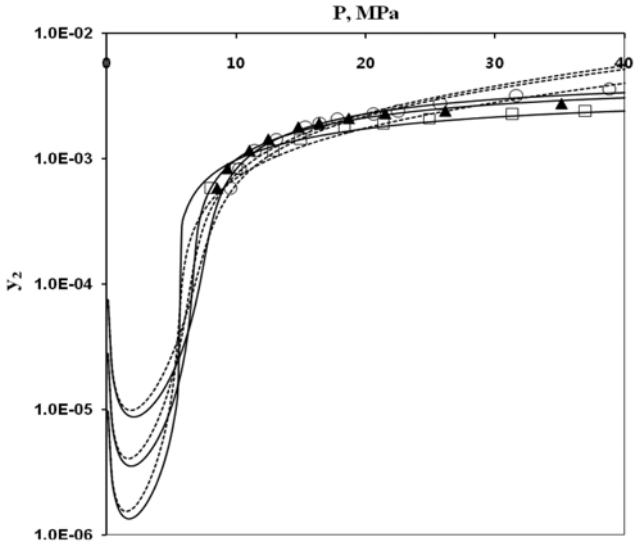

Fig. 4. Solubility of hinokitiol in supercritical ethane with the PR (dotted line) and QLF (solid line) EOS: □, 313.2 K; ▲, 323.2 K; ○, 333.2 K.

CONCLUSION

The equilibrium solubility of hinokitiol in supercritical carbon dioxide and ethane was measured using a variable volume view cell in the pressure range from 8 to 40 MPa and at temperatures equal to 313.2, 323.2 and 333.2 K. The experimental data were correlated by the PR EOS and the QLF EOS. The QLF EOS fits better experimental data in carbon dioxide+hinokitiol and ethane+hinokitiol systems than the PR EOS because the critical properties for hinokitiol in PR EOS were estimated from group contribution method. Meanwhile, near the critical region these models could not describe quantitatively the experimental data in both systems. Therefore, the experimental data of biomaterials in supercritical fluids is essential in successive modeling phase behavior near the critical region.

ACKNOWLEDGEMENT

This paper was supported by Eulji University in 2010.

NOMENCLATURE

A : Helmholtz free energy
k : Boltzmann's constant
q : surface area parameter
r : number of segments per molecule
T : temperature
T^* : characteristic temperature
p : pressure
p^* : characteristic pressure

V : volume
v : molar volume
v^* : close packed volume of a r-mer
x : liquid mole fraction
z : lattice coordination number
Z : compressibility factor

Greek Letters

β : reciprocal temperature [1/kT]
ε_{ij} : molecular interaction energy
ε_M : defined by Eq. (13)
φ : fugacity coefficient
ρ : molar density
ρ^* : close packed molar density
θ : surface area fraction

REFERENCES

1. S. E. Byeon, Y. G. Lee, J. C. Kim, J. G. Han, H. Y. Lee and J. Y. Cho, *Planta Med.*, **74**, 828 (2008).
2. N. Komaki, T. Watanabe, A. Ogasawara, N. Sato, T. Mikami and T. Matsumoto, *Biol. Pharm. Bull.*, **31**, 735 (2008).
3. K. D. Manter, R. G. Kelsey and J. J. Karchesy, *J. Chem. Ecol*, **33**, 2133 **(**2007).
4. K. Murakami, Y. Ohara, M. Haneda, R. Tsubouchi and M. Yoshino, *Basic Clin. Pharmacol. Toxicol.*, **97**, 392 (2005).
5. S. Liu and H. Yamauchi, *Cancer Lett.*, **286**, 240 (2009).
6. D. S. Kim, S. H. Park, S. B. Kwon, K. Li, S. W. Youn and K. C. Park, *Arch. Pharm. Res.*, **27**, 334 (2004).
7. T. Baba, H. Nakano, K Tamai, D. Sawamura, K. Hanada, I. Hashimoto and Y. Arima, *J. Invest. Dermatol.*, **110**, 24 (1998).
8. A. S. Teja and C. A. Eckert, *Ind. Eng. Chem. Res.*, **39**, 4442 (2000).
9. J. Rincón, F. Martínez, L. Rodríguez and V. Ancillo, *J. Supercrit. Fluids*, **56**, 72 (2011).
10. M. A. McHugh, A. J. Seckner and T. J. Yogan, *Ind. Eng. Chem. Fundam.*, **23**, 493 (1984).
11. R. T. Kurnik, S. J. Holla and R. C. Reid, *J. Chem. Eng. Data*, **26**, 47 (1981).
12. K. Schafer and W. Baumann, *Fres. Z. Anal. Chem.*, **332**, 122 (1988).
13. R. D. Weinstein, W. H. Hanlon, J. P. Donohue, M. Simeone, A. Rozich and K. R. Muske, *J. Chem. Eng. Data*, **52**, 256 (2007).
14. J. F. Brennecke and C. A. Eckert, *AIChE J.*, **35**, 1409 (1989).
15. M. Škerget, Z. Novak-Pintarič, Ž. Knez, Z. Kravanja, *Fluid Phase Equilib.*, **203**, 111 (2002).
16. J. Cheng, M. Tang and Y. Chen, *Fluid Phase Equilib.*, **194-197**, 483 (2002).
17. C. Nicolas, E. Neau, S. Meradji and I. Raspo, *Fluid Phase Equilib.*, **232**, 219 (2005).
18. M. S. Shin and H. Kim, *Fluid Phase Equilib.*, **246**, 79 (2006).
19. M. S. Shin and H. Kim, *Fluid Phase Equilib.*, **256**, 27 (2007).
21. M. S. Shin and H. Kim, *J. Chem. Thermodyn.*, **40**, 1110 (2008).
21. M. S. Shin, J. H. Lee and H. Kim, *Fluid Phase Equilib.*, **272**, 42 (2008).
22. M. S. Shin and H. Kim, *Fluid Phase Equilib.*, **270**, 45 (2008).
23. M. S. Shin and H. Kim, *Clean Technol.*, **14**, 153 (2008).
24. C. I. Park, M. S. Shin and H. Kim, *J. Chem. Thermodyn.*, **41**, 30 (2009).
25. D.-Y. Peng and D. B. Robinson, *Ind. Eng. Chem. Fundam.*, **15**, 59 (1976).
26. W. Bae, S. Kwon, H. S. Byun and H. Kim, *J. Supercrit. Fluids*, **30**, 127 (2004).
27. S. E. Stein and R. L. Brown, *J. Chem. Inf. Comput. Sci.*, **34**, 581 (1994).
28. W. J. Lyman, W. F. Reehl and D. H. Rosenblatt, Handbook of Chemical and Physical Property Estimation Methods: Environmental Behavior of Organic Compounds, *American Chemical Society*, Washington, D.C. (1990).
29. R. F. Fedors, *Polym. Eng. Sci.*, **14**, 147 (1974).
30. J. Kang, K. P. Yoo, H. Kim, J. Lee, D. Yang and C. S. Lee, *Int. J. Thermophys.*, **22**, 487 (2001).